DE-Vol. 69-2, Advances in Design Automation – 1994
Volume 2
ASME 1994

"CHAOS" BY DESIGN IN MOBILE ROBOTS

Arulkumar P. Shanmugasundram and S. Desa
Sibley School of Mechanical and Aerospace Engineering
Cornell University
Ithaca, New York

ABSTRACT

A large class of tasks for mobile robots require the robot to cover an enclosed space that might contain several objects (obstacles). The usual approach to this problem is to design a sensor-intensive, computer-controlled robot that usually has a relatively simple kinematic form (type). The control of such a robot is difficult, expensive, and frequently unreliable. This paper demonstrates how the complexity in sensing and control can be circumvented by synthesizing a "chaotic" kinematic motion that, when appropriately embodied by a kinematic form, covers the space and easily deals with obstacles. The evolution of the "chaotic", sensorless, mechanical mobile robot from concept, through analysis, numerical simulation and form embodiment, to realization is described. The testing of the prototype clearly demonstrates how, for the present task, complex "chaotic" motions do considerably simplify the control of the robot. A computer controlled prototype capable of mimicking the behavior of its mechanical counterpart is also described.

1. INTRODUCTION

In this paper we address a fundamental question in the design of autonomous mobile robots. Can one simplify the control of the robot by suitably designing its form (kinematic type, kinematic structure)? This question is addressed in the context of a complex task which typifies of a large class of applications: navigating in ("covering") an enclosed space which contains several objects (that must be avoided). A practical example of such a task is the design of a mobile robot to autonomously vacuum-clean the floor of a room. We demonstrate analytically and experimentally how the control of a mobile robot can be considerably simplified by the intentional introduction of a suitable discontinuity in the kinematic motion and corresponding form ("type") of the robot. In the particular case studied in this paper the discontinuity results in "chaotic" behavior which enable the mobile robot to deal relatively easily with the objects in the workspace.

A straight-forward and widely used solution to the problem of covering an enclosed space is to build a platform with two independent, single degree-of-freedom, computer-controlled drive wheels. By suitable selection and control (open-loop or closed-loop) of the angular velocity of each drive wheel the robot can be suitably programmed to cover the prescribed space. However this mechanical form has considerable difficulty in dealing with obstacles and usually requires very complex motion planning strategies, for example, the use of potential fields [Khatib, 1986] to properly navigate in an obstacle field. It is clear that the simple motion capability at each wheel and resulting simple kinematic form is offset by the complexity in controlling the device(to perform its task). This observation leads us to pose the following important design problem:

Synthesize a complex kinematic motion and resulting kinematic form that considerably simplifies the control of the machine.

The approach taken to resolving the above problem is based on the observation that deterministic systems with relatively simple structure can, by suitable input excitation, be made to exhibit so-called chaotic motions [Moon,F.C., 1992]. These chaotic motions have two properties which serve as the basis for the mobile robot design:

(i) they tend to "fill" or "cover" a space,

(ii) the random nature of the motion enables wall and objects (obstacles) to be treated as merely additional sources of randomness that do not require the use of complex, control strategies for dealing with them.

We now describe how, starting with the above premise, the design [Pahl and Beitz, 1992] of a "chaotic" mobile robot evolved from concept through embodiment of form to actual realization and testing.

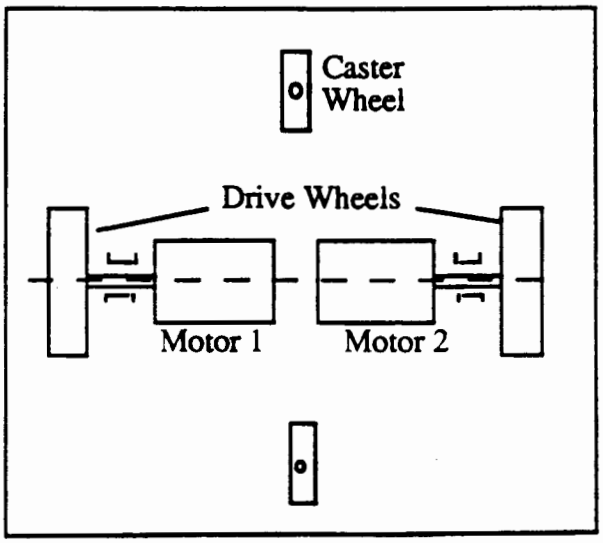

FIGURE 1 A COMPUTER CONTROLLED MOBILE ROBOT

2. OUTLINE OF THE PAPER

The design of the mobile robot can be decomposed into the following steps:

(i) Synthesize a "chaotic" kinematic motion that by its very nature covers the space.

(ii) Let the robot "interact" with the obstacles rather than try to explicitly avoid them. (Interaction with obstacles will be defined and addressed in more detail, later). The interaction with the obstacle will simply cause the robot to move in some new direction that does not adversely affect, and might even aid, the "chaotic" motion. The problem of dealing with obstacles is therefore resolved in a relatively simple fashion.

(iii) Synthesize a kinematic form (type) that realizes the motion synthesized in step (i).

(iv) Develop and test suitable realizations of the kinematic form.

In the next section we synthesize a kinematic motion that covers the space and deals with obstacles. In section 4 we develop both mechanical and programmable ways of achieving the desired motion. The actual realization of the robot is then discussed in Section 5. Finally in Section 6 we briefly summarize the results, draw relevant conclusions and discuss work in progress.

It is important to note that separation of the kinematic motion synthesis from the kinematic form synthesis is essential in order to generate both mechanical and mechatronic concept variants [Pahl and Beitz, 1992] for achieving "chaotic" motion.

3. MOTION SYNTHESIS

In order to develop a device that displays chaotic motion, we start with a simple wheel B rolling on a horizontal plane. For the present purposes the wheel, which is vertical, has two inputs $\dot{\theta}$ and $\dot{\varphi}$, where θ and φ are the two angles shown in Figure 2.

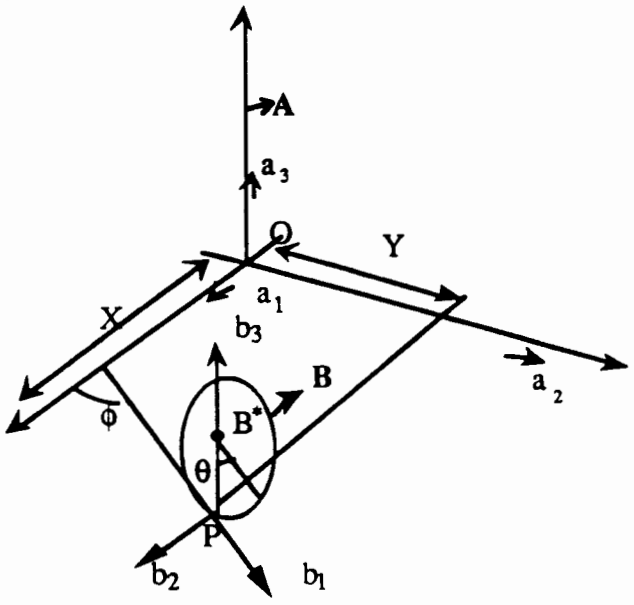

FIGURE 2 MOTION OF THE WHEEL

The actuator which produces the input $\dot{\theta}$ is called the drive actuator, and the actuator which produces the input $\dot{\varphi}$ is called the steering actuator. The magnitude of $\dot{\varphi}$ is generally much less than that of $\dot{\theta}$. If $\dot{\varphi}$ and $\dot{\theta}$ are constant, then the trajectory of the mass center B^* of B, when B rolls without slipping on a plane (see Figure 2), and the wheel is always vertical, is a circle. In the analysis below $\dot{\theta}$ is a constant.

A model is chosen to generate equations that provide behavior that covers the whole space. One such model is to have rotations of two different scales and introduce a discontinuity. A graphical representation of the model is shown in Figure 3.

3.1 Motion in the absence of wall and object constraints

Consider a simple wheel B which can rotate about two orthogonal axes passing through its center of mass B^* and parallel to unit vectors $\vec{b}_2$ and $\vec{b}_3$ fixed in B. Let A be a fixed reference frame and let $\vec{a}_1, \vec{a}_2, \vec{a}_3$ be a dextral orthogonal set of unit vectors fixed in A. The angular velocity $\vec{\omega}$ of B in A can be written as

$$\vec{\omega} = \dot{\theta}\vec{b}_2 + \dot{\varphi}\vec{b}_3 \tag{1}$$

In our case both $\dot{\theta}$ and $\dot{\varphi}$ are specified functions of time (there is an actuator causing the specified angular speed about each axis). Therefore, only two generalized co-ordinates (X,Y) are necessary to describe the configuration of B in A (see Figure 2).

The velocity $\vec{V}$ of the mass center B^* of B in A can be written as

$$\vec{V}^{B^*} = \dot{X}\vec{a}_1 + \dot{Y}\vec{a}_2 \tag{2}$$

Let P denote the point of B that is in contact with the horizontal plane at the instant of interest. If B rolls on the horizontal plane then

$$\vec{V}^{P} = 0 \tag{3}$$

It can be easily shown that the condition (3) gives rise to the following equations:

$$\dot{X} = r\dot{\theta}(t)\cos(\varphi(t)) \tag{4}$$

$$\dot{Y} = r\dot{\theta}(t)\sin(\varphi(t)) \tag{5}$$

Let the angular displacement $\varphi(t)$ be produced by an input angular displacement $\psi(t)$ and let the relationship between $\varphi(t)$ and $\psi(t)$ be as shown in Figure 3. Furthermore, let

$$\psi = \alpha t \quad (\Rightarrow \dot{\psi} = \alpha) \tag{6}$$

where α is the constant angular speed of the input. From Figure 3 we see that $\dot{\varphi}$ is a discontinuous periodic function given by

$$\dot{\varphi} = 0 \qquad n(2\pi) < \alpha t < n(2\pi) + \beta \tag{7}$$

$$= \alpha \qquad n(2\pi) + \beta < \alpha t < (n+1)2\pi \text{ , } (n=0,1,2,....) \tag{8}$$

The angle β in Figure 3 will be referred to as the dwell angle. During the time corresponding to the dwell angle the steering rate, $\dot{\varphi}=0$, i.e. the wheel moves in a straight line.

If we define,

$$\varphi(i) \equiv \varphi(t=iT) \tag{9}$$

where $T = 2\pi/\alpha$. Then from Figure 3

$$\varphi(i) = \varphi(0) + i(2\pi - \beta) \tag{10}$$

Without loss of generality we will assume, that

$$\varphi(0) = 0 \tag{11}$$

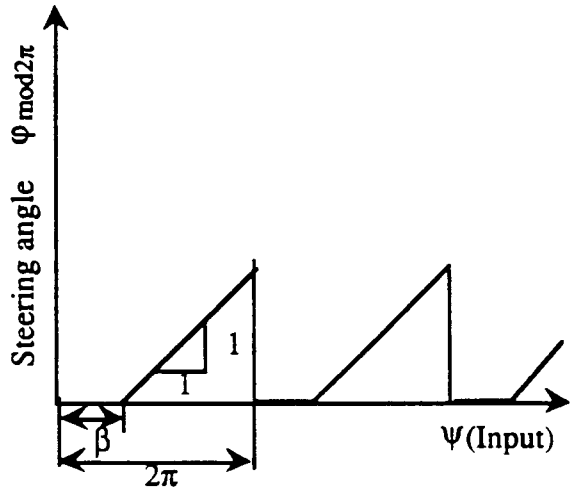

FIGURE 3. STEERING ANGLE AS FUNCTION OF INPUT

If (X(0), Y(0)) denotes the initial position of the mass center B^* in A and (X(n), Y(n)) the position of the mass center B^* in A at t=nT, then one can show that

$$X(1) = X(0) + r\dot{\theta}\cos(\varphi(0))\frac{\beta}{\alpha} + \frac{r\dot{\theta}}{\alpha}\left\{\sin(\varphi(0)) - \sin(\varphi(0)+\beta)\right\} \tag{12}$$

$$Y(1) = Y(0) + r\dot{\theta}\frac{\beta}{\alpha}\sin(\varphi(0)) + r\frac{\dot{\theta}}{\alpha}\{\cos(\beta+\varphi(0))-\cos(\varphi(0))\} \quad (13)$$

By the same argument, the position of B^* after nT seconds is given by,

$$X(n) = X(n-1) + r\dot{\theta}\cos(\varphi(n-1))\frac{\beta}{\alpha} + r\frac{\dot{\theta}}{\alpha}\{\sin(\varphi(n-1))-\sin(\varphi(n-1)+\beta)\} \quad (14)$$

$$Y(n) = Y(n-1) + r\dot{\theta}\frac{\beta}{\alpha}\sin(\varphi(n-1)) + r\frac{\dot{\theta}}{\alpha}\{\cos(\beta+\varphi(n-1))-\cos(\varphi(n-1))\} \quad (15)$$

From equations (14) and (15) one can easily see that if $\beta=0$, i.e., the output φ is a continuous linear function of the input ψ (in Figure 3), then

$$X(n)=X(n-1) \quad (16)$$

$$Y(n)=Y(n-1) \quad (17)$$

which means that as stated earlier, the trajectory of the mass center B^* is a circle.

Combining equations (12) and (14) and using recursion we can write,

$$X(n) = X(0) - r\frac{\dot{\theta}}{\alpha}\sin(\beta) + \sum_{i=0}^{n-1} r\dot{\theta}\frac{\beta}{\alpha}\cos(\beta i) - r\frac{\dot{\theta}}{\alpha}\sin(\beta(n-1)) \quad (18)$$

Similarly, combining equations (13) and (15) and using recursion we can write,

$$Y(n) = Y(0) + r\frac{\dot{\theta}}{\alpha}\cos(\beta) - \sum_{i=0}^{n-1} r\dot{\theta}\frac{\beta}{\alpha}\sin(\beta i) - r\frac{\dot{\theta}}{\alpha}\cos(\beta(n-1)) \quad (19)$$

Equations (18) and (19) describe the mapping between the initial position (X(0),Y(0)) and the position after n periods. From these equations we can make the following observations:

(1) If β is measured in degrees and $360/\beta$ is rational, then the motion of B^* is periodic. If p denotes the periodicity of the motion, i.e.

$$X(p+n) = X(n)$$
$$Y(p+n) = Y(n),$$

then, $$p=360/HCF(360,\beta) \quad (20)$$

where HCF(360,β) is the highest common factor of 360 and β.

(2) If $360/\beta$ is irrational, the motion of B^* is quasi-periodic.

3.1.1 Simulations

It is useful to describe the kinematic motion of the wheel by three states X,Y and φ whose evolution in time (flow) is described by the differential equations (4), (5), (7) and (8). In order to understand and characterize the motion of the mobile robot the following numerical simulations were performed:

1. The trajectory (X(t),Y(t)) of the mass center B^* obtained by numerically integrating equations (4), (5), (7) and (8).
2. The discrete map corresponding to the position (X(n),Y(n)) of the mass center B^* at t=nT seconds. (X(n),Y(n)) are also given, respectively by equations (18) and (19).

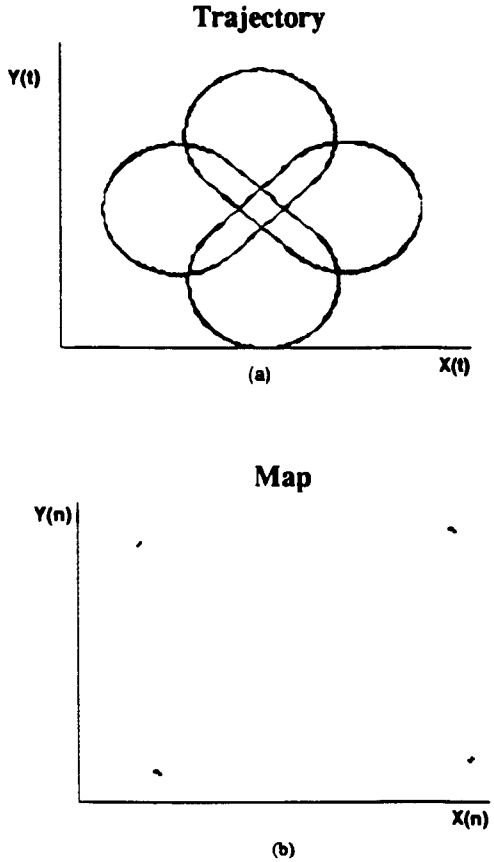

FIGURE 4 MOTION OF THE MASS CENTER FOR DWELL ANGLE =90°

The trajectory and corresponding map of B^* for rational dwell angles $\beta=90^\circ$ and 18° are shown, respectively in Figures 4 and 5.

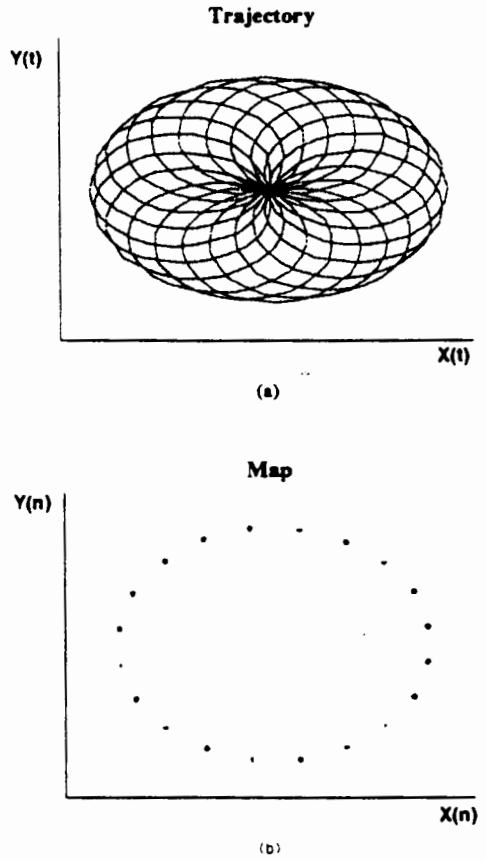

FIGURE 5 MOTION OF THE MASS-CENTER FOR DWELL ANGLE =18°

The trajectory and map of B^* for the case when the dwell angle β is irrational ($= (\frac{(\sqrt{5}-1)}{2} * 90^\circ$) is shown in Figure 6.

For each simulation the initial state of the device is (0,0,0), $\dot{\theta}$=6.5 rad/sec, α=0.628 rad/sec. The simulations shown in Figure 6 were run for 800 seconds. The radius of the wheel is 0.25 feet (=0.0625m).

From the above simulations the following useful observations emerge:

1. By appropriate choice of β and the ratio $(\dot{\theta}/\alpha)$ it is possible for B^* (and therefore the wheel) to cover a space of any size.

2. As predicted by equations (18), (19), the maps corresponding to rational dwell angles (Figure 4(a),(b)) are periodic with periodicity given by equation (20).

3. The map shown in Figure 6 (b), corresponding to the irrational dwell angle, clearly reveals the expected quasi-periodic nature of the motion. Note how densely the corresponding trajectory covers the space. If the simulations were run for a longer period of time the corresponding map(see figure 6b) would cover a circle.

4. The simulation results of Figures 4, 5 and 6 indicate that a small rational dwell angle tends to approach the space-covering property of an irrational dwell angle.

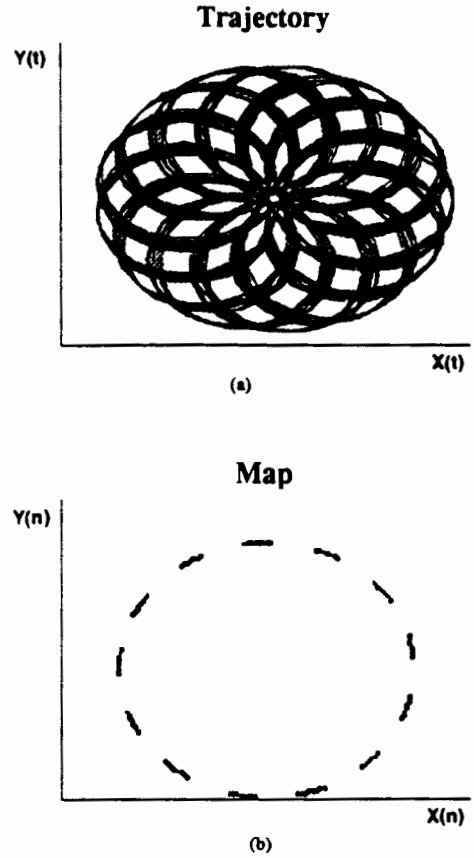

FIGURE 6 MOTION OF THE MASS-CENTER FOR AN IRRATIONAL DWELL ANGLE

3.2 Motion in the presence of wall and object constraints

We allow the wheel (robot) to make contact with the wall and model the interaction between the wheel and the wall as follows. When the wheel touches the wall, the mass center B^* essentially stops moving. The wheel "precesses" about the vertical axis at the rate $\dot{\varphi}=\alpha$ until

the vector $\vec{b}_1$ (see Figure 2) is parallel to the wall at which point the wheel moves parallel to the wall. (This model is consistent with experimental observations (see Section 5) for an actual robot (wheel) moving at moderate speed and lightly impacting a wall.

A simulation of the motion of the mass center B^* of the robot moving in a rectangular walled space is shown in Figure 7 (a) and 7(b). The simulations are done in a room of size 10 feet x10 feet with a dwell angle of 18 degrees and for a time period of 800 seconds. These simulations are performed by treating the wheel as a point in its configuration space (Lozano-Perez, 1983).

In the simulations shown in Figure 7, in order to cover the whole space, the ratio $\dot{\theta}/\dot{\varphi}$ is chosen such that $r^*\dot{\theta}/\dot{\varphi}$ is a little greater than half the largest dimension of the room .

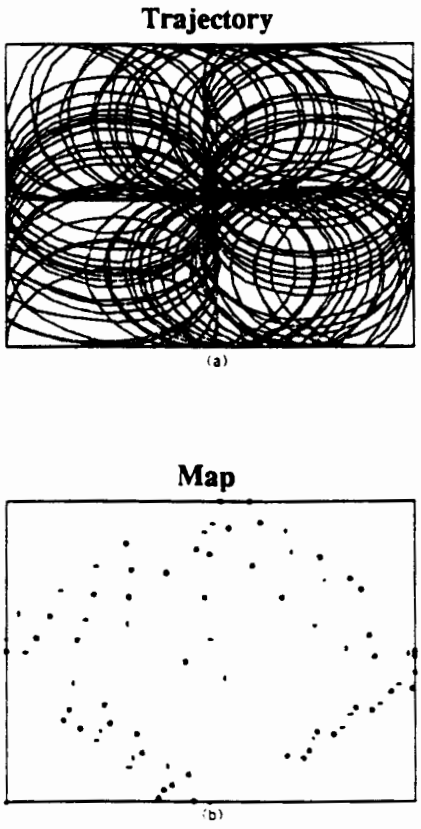

FIGURE 7 MOTION OF THE MASS-CENTER IN THE PRESENCE OF WALLS

The next step is to study the effect of obstacles in the workspace. If the wheel is permitted to lightly impact the obstacles then the interaction between the wheel and the obstacle is modeled as in the case of the wall. A simulation of the motion of the mass center of the robot moving in a rectangular walled space which contains two obstacles is shown in Figures 8(a) and 8(b).

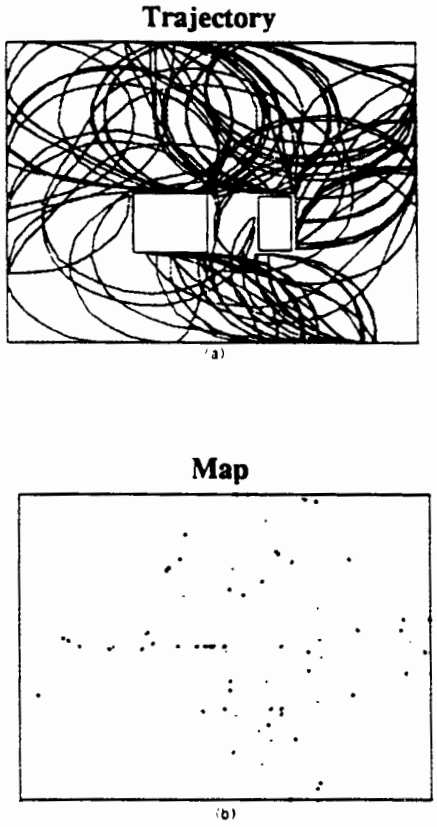

FIGURE 8 MOTION OF THE MASS-CENTER IN THE PRESENCE OF WALLS AND OBSTACLES

From Figures 7 and 8 we see that the presence of walls and obstacles make the motion of B^* (and therefore, the robot) "chaotic", which is what is desired. Furthermore, the robot simply takes the walls and obstacles in its "stride" and does not require any complicated obstacle avoidance/motion planning strategy.

3.3 "Chaos"

An explanation of the use of the word "chaotic" in the present context is in order. To this end, two more sets of simulations were done. The results of the first set of simulations (Figure 9) show the sensitivity of the

trajectory of B^* to initial conditions for the following two cases:

(i) The wheel moves in an open space(the dashed line in Figure 7).

(ii) The wheel moves in an enclosed (i.e., walled) space. (the solid line in Figure 7).

In each case the initial state φ was given a small perturbation and the magnitude of the resulting perturbation in the trajectory of B^* was computed and plotted as a function of time (Figure 9). While the trajectory of B^* in an open space is not sensitive to initial conditions, the corresponding trajectory in the enclosed(walled) space displays considerable sensitivity to initial conditions.

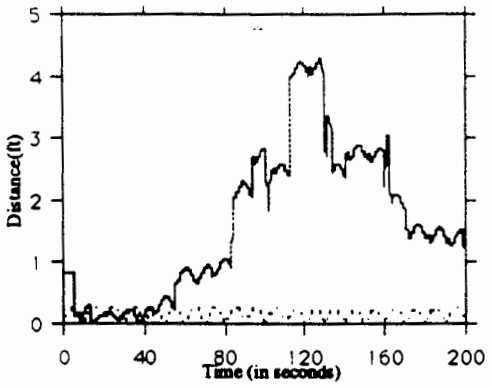

FIGURE 9. SENSITIVITY TO INITIAL CONDITIONS

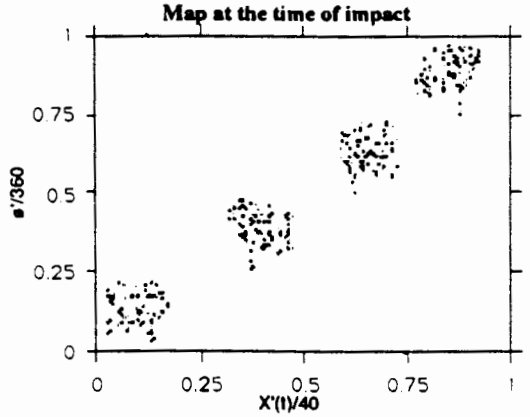

FIGURE 10 IMPACT MAP

The second simulation, shown in Figure 10, is an impact map which is obtained by determining X' and φ', where X' represents the point on the unfolded wall perimeter where the wheel makes impact with the wall and φ' (in degrees) is the corresponding steering angle at the time of impact. (The coordinate X' is normalized w.r.t. the perimeter of the room = 40 feet, and the angle φ' (degrees) is normalized with respect to a full revolution). Each point in Figure 10 therefore represents a point of impact. The clustering of the points along the diagonal indicates that the wheel "visits" each wall at several points along the length of the wall.

While the motion of the wheel for the case of obstacle constraints (Figure 8) is not chaotic in the classical sense [Moon,1992;Ottino,1989] it is

(a) obtained from a simple deterministic set of differential equations.

(b) is sensitive to initial conditions (Fig. 9) and

(c) it displays complex ("chaotic") behavior (Figures 8 and 10). We have therefore decided to call the observed behavior "chaotic".

In summary, we have shown that a wheel driven at a constant rate $\dot{\theta}$ and with a discontinuous steering input $\dot{\varphi}$ will, in the presence of obstacles (walls and objects), exhibit a "chaotic" motion which effectively covers the space and easily deals with obstacles.

4. FORM SYNTHESIS

In order to develop a kinematic form capable of realizing the chaotic motion synthesized above, two issues must be resolved. The first issue is the implementation of the input-output motion described by equations 7 , 8 and shown in Figure 3. The second issue is the interaction of the robot with obstacles.

One method of implementing the desired kinematic motion is shown in Figure 11. Motor 1, called the drive motor (see figure 11(a)), essentially "supplies" the constant angular speed $\dot{\theta}$ which propels (drives) the wheel (or robot). Motor 2, acting through a pair of gears labeled input gear and output gear, "supplies" the time-dependent, discontinuous, periodic angular speed $\dot{\varphi}$. In order to obtain the desired input-output kinematic motion shown in figure 3, the input gear must be "mutilated" as shown in Figure 11(b), by an amount equal to the dwell angle β. The output gear(and, therefore, the shaft which causes the vertical rotation φ of the wheel) will then have the desired output motion shown in Figure 3. Another method of obtaining the

necessary dwell is to use a six-bar linkage which has a(n) (approximate) single dwell: the input-output relationship in this case would be discontinuous.

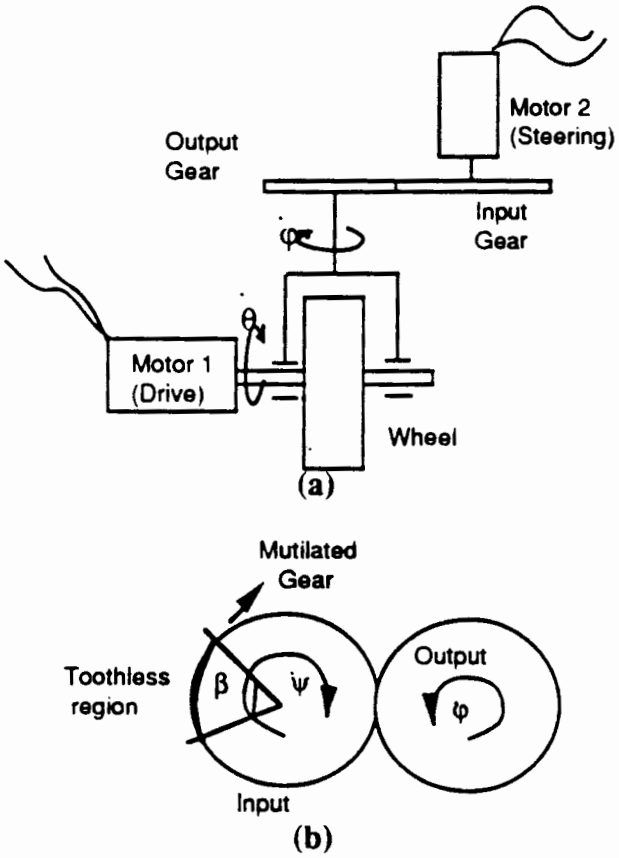

FIGURE 11. SCHEMATIC OF A MOBILE ROBOT

The required output motion $\dot{\varphi}(t)$ can also be obtained by suitably programming the computer controlled mobile robot shown in Figure 1. If the appropriate angular velocity command is given to each drive wheel, then the robot in Figure 1 can be made to mimic the single drive-wheel robot of Figure 11. We can therefore program the robot of Figure 1 to have a single "virtual" drive wheel with any desired steering motion (for example, the steering motion φ shown in Figure 3).

The basic obstacle interaction strategy, as mentioned earlier, is to let the robot lightly impact the obstacle causing the drive motor(motor 1) to stall. The steering motor then turns the wheel till it is free to move in a direction parallel to the tangent to the obstacle surface at the point of contact (impact). To keep the motor from stalling between the time when the robot impacts the obstacle and the time when it is free to move, a slip clutch, which permits the motor shaft to spin freely w.r.t. the wheel shaft if the load torque from the wheel exceeds a specified magnitude, must be inserted between the motor shaft and the wheel shaft. In order to further facilitate the interaction of the robot with obstacles the base of the robot can be made circular in shape as shown in Figure 12.

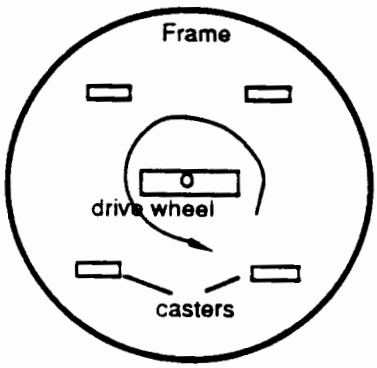

FIGURE 12. PLAN VIEW OF THE ACTUAL MOBILE ROBOT

In the case of the computer controlled implementation (Figure 1), the robot can be programmed to interact with the obstacle in a manner similar to that described above. Furthermore, additional sensing (using sonar, for example) can be advantageously used to ensure that while the robot gets close to the obstacle, it does not make actual contact.

5. REALIZATION AND TESTING

A systematic design process [Pahl and Beitz, 1992] was used to develop two actual mobile robot prototypes based on the ideas developed in Sections 3 and 4. One prototype uses the kinematic form shown in Figure 11 and is discussed in more detail below. The other prototype is the computer-controlled mobile robot that is shown schematically in Figure 1 and that is currently being programmed to mimic the behavior of the mechanical implementation. The design of both the prototypes is comprehensively documented in the report [MAE 425, Fall 1993].

The realization of the mechanical implementation (see Figures 11(a),(b)) of the "chaotic" mobile robot is shown in Figure 13. The robot has a single drive wheel with two independently driven axes as shown in Figure 11(a). Four caster wheels (see Figure 12) are used to provide additional support for the platform which supports the payload (in this case a vacuum cleaning

unit) carried by the robot. A slip clutch between the drive motor and the drive wheel prevents the drive motor from stalling whenever the robot hits a wall or an obstacle. Figure 14 is an exploded view showing the relative placement of the components that make up the drive wheel assembly (drive motor, slip clutch, etc.). The circular shape of the platform facilitates the navigation of the robot near the walls, corners, and obstacles. A spring loaded bumper minimizes the impact forces on the robot during interaction with the object.

FIGURE 13 "CHAOTIC" MOBILE ROBOT

To test the robot the following task was defined: clean a 12x20 foot room which has several objects in it. To determine how well the robot covered the space (i.e. cleaned the room) the floor was covered with little bits of paper. The robot was then set in the room and allowed to move. The following results were obtained:
1)The robot motion was very "chaotic".
2)The robot had no difficulty dealing with obstacles, walls or corners.
3)The room was quite thoroughly cleaned in five minutes. The chaotic motion was therefore very effective in covering the space.

The robot was tested several times with different initial conditions. (A videotape of the robot performing its task is available for inspection). From the results of the test we can conclude that the "chaotic" mobile robot effectively covers the space and deals with obstacles as predicted by the analysis in Section 3.

6. SUMMARY AND CONCLUSIONS

In Section 3 we showed that a simple discontinuous kinematic steering motion (Figure 3) containing a dwell period, in conjunction with walls and obstacles, leads to the "chaotic" motion of a driven wheel. A mutilated gear form (Figure 11 b) was used to obtain the required dwell period. Finally, in order to demonstrate the feasibility of using "chaotic" motions to perform useful tasks, an actual prototype was realized and successfully tested.

A second computer controlled prototype has also been built and will be programmed to perform the task (covering an enclosed space which contains obstacles) by mimicking the mechanical design described in Section 5. This programmable machine, once it successfully performs its task, will have the added advantage-at the expense of additional sensing-of avoiding contact with obstacles. The completely mechanical prototype demonstrates the premise that the appropriate synthesis of a relatively complex (in the present case, "chaotic") kinematic motion and its corresponding kinematic form results in a mobile robot which is easy to control.

ACKNOWLEDGMENTS

Professor Francis C. Moon provided a perspective on modern nonlinear dynamics which was useful in shaping the present work. Discussions with Vivek Bhatt, Brian Coller, Matthew Davies and George Muntean provided useful insights on chaos in physical systems that were relevant to our work. The design of the "chaotic" robot was carried out within the context of the Senior Design Course MAE 425 at Cornell University.

REFERENCES

Kane, T. R. and Levinson, D. A., 1985, Dynamics: Theory and Applications, McGraw-Hill Inc..

Khatib,O, 1986, "Real-time obstacle avoidance for robot manipulators and mobile robots", The

International Journal of Robotics Research, Vol. 5, No. 1, pages 90-98.

Lozano-Perez, T., 1983, "Spatial Planning: A configuration space approach", IEEE Transactions on Computers, C-32(2)., pages 108-120

MAE 425 Project Report, Fall 1993, Sibley School of Mechanical and Aerospace Engineering, Cornell University.

Moon, Francis C., 1992, Chaotic and Fractal Dynamics, John Wiley & Sons, Inc.

Ottino, J. M., 1989, The kinematics of mixing: stretching, chaos and transport, Cambridge University Press.

Pahl G and Beitz W, 1992, Engineering Design: A Systematic Approach, Springer-Verlag.

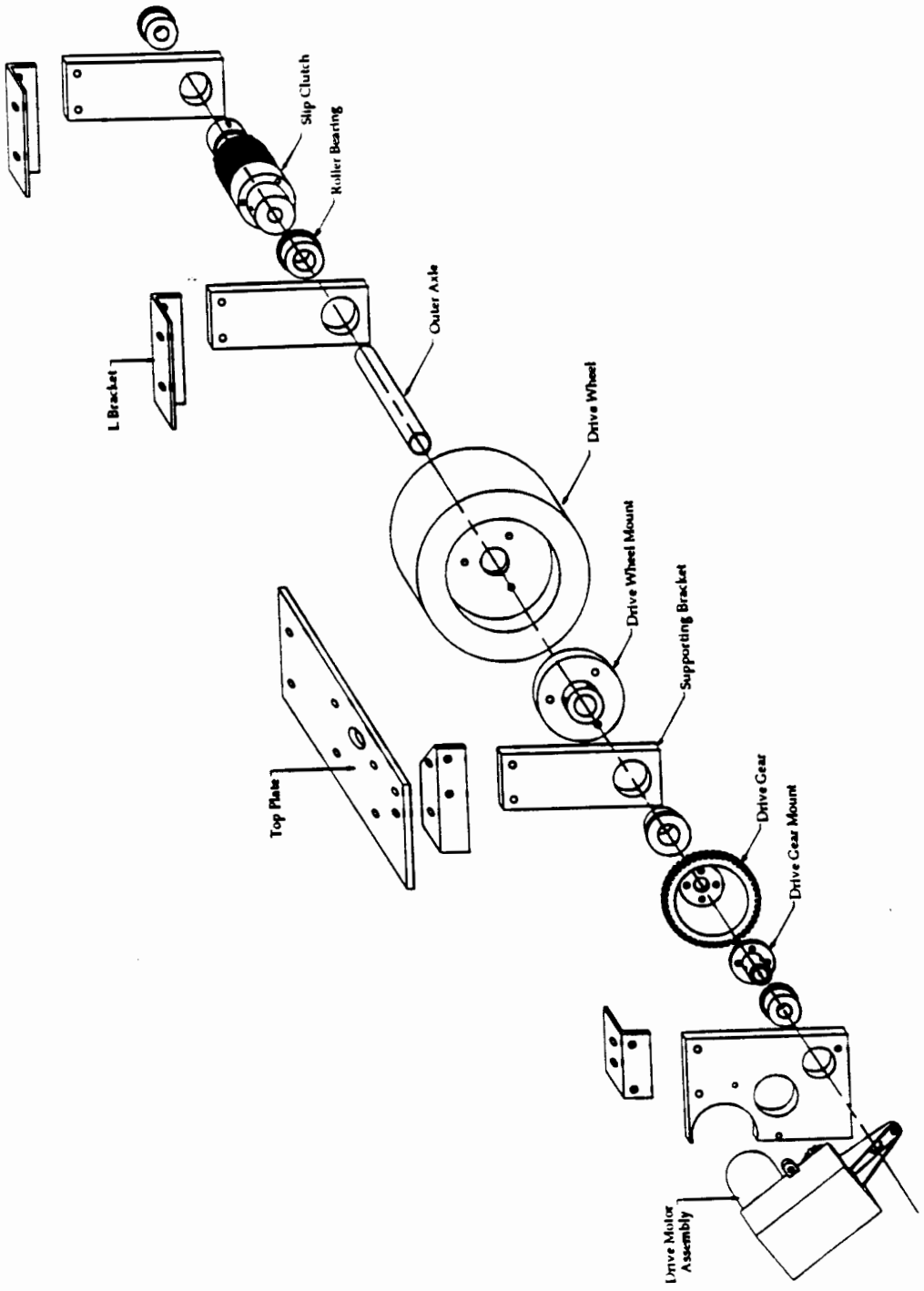

FIGURE 14. EXPLODED VIEW OF THE DRIVEWHEEL ASSEMBLY